ISTITUTO NAZIONALE DI FISICA NUCLEARE

Sezione di Torino

Roberto Chierici

W PRODUCTION AND m_W MEASUREMENT USING THE DELPHI DETECTOR AT LEP

W PRODUCTION AND m_W MEASUREMENT USING THE DELPHI DETECTOR AT LEP

Roberto Chierici
Dipartimento di Fisica Sperimentale, Università di Torino and INFN,
Via P.Giuria 1, 10125 Torino

Abstract

During LEP 1996 runs at centre of mass energies of 161 GeV and 172 GeV the DELPHI detector collected data corresponding to an integrated luminosity of approximately 20 pb^{-1}. At these energies W pair production events were observed in all possible final states allowing a measurement of the cross section $\sigma(ee \rightarrow WW)$. The mass of the W boson was also extracted using the cross section value at threshold and by direct reconstruction at 172 GeV. In this document the event selection criteria and the W mass measurement methods are briefly described; the final DELPHI results at 161 GeV and preliminary results at 172 GeV on m_W and σ_W^{CC03} are presented.

1 Introduction

W boson pair production and study is one of the main physics goals of LEP2. The measurement of WW production cross section and the determination of limits for the anomalous three boson couplings are two of the most relevant subjects in W physics at LEP2 energies, but special importance must be given to the precise determination of the W mass. In fact, m_W is a fundamental parameter of the Standard Model, so far directly measured only at CERN and Fermilab Tevatron $p\bar{p}$ colliders [1], [2], [3], [4]. The non-LEP world average W mass is, at present:

$$m_W = 80.356 \pm .125(exp) \ \text{GeV}/c^2 \tag{1}$$

The foreseen precision which can be obtained at LEP2 on m_W assuming a luminosity of 500 pb^{-1} per experiment is about 35 MeV/c^2 [5]. Such a precise determination of m_W, compared with the value derived from a fit to all known electroweak parameters, will represent a new test of the Standard Model and could as well give valuable information on the Standard Higgs boson mass. [6]

This document reports on the first m_W measurement using the DELPHI detector at LEP and is organized as follows: after a brief introduction on W production mechanism and on LEP2 schedule, description and performances of W selection criteria used in DELPHI are presented. The techniques to measure WW cross sections and W mass are then described and the results on those measurement, which are final at $\sqrt{s}$= 161 GeV and preliminary at $\sqrt{s}$ = 172 GeV, are reported. Combination of results and conclusions follow.

2 W Production in e$^+$e$^-$ annihilations at LEP2 energies.

2.1 W pair production and LEP2

W pair production through e$^+$e$^-$ annihilation is possible via two s-channel diagrams and one t-channel diagram which are shown in figure 1 and constitute the so called CC03 processes. The total cross section for such diagrams is shown in the left plot of figure 2: a sharp increase of the cross section is evident above the threshold of W pair production ($\sqrt{s}$=2m_W) which is smeared out by finite W width effects and initial state radiation. In the right part of figure 2 the same cross section is presented, but with a different scale of energies and for different values of m_W. The cross section sensitivity to m_W can therefore be used at threshold to extract the second from a measurement of the first. This method is expected to give less precision in the determination of m_W than the method of direct reconstruction, used at higher energies, but has the advantage to be completely independent and to have different systematics which makes it possible to use it as a reliable crosscheck for the direct measurement. Furthermore, the idea of spending some luminosity of LEP2 at the W threshold region fitted well into the LEP2 program to reach higher energies in several steps with the installation of more radiofrequency cavities in the tunnel.

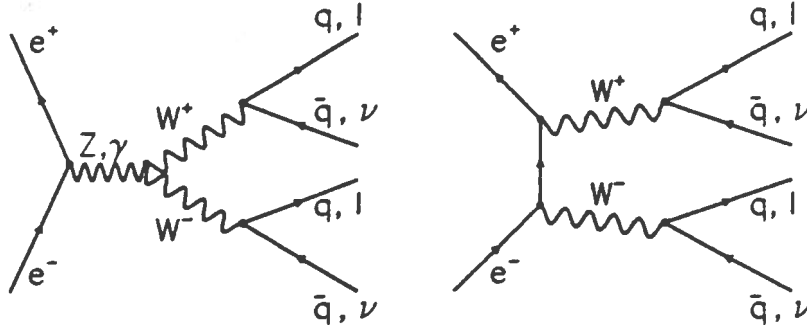The tuning of the energy in the threshold region was optimized in order to minimize

Figure 1: s channel and t channel W boson pair production diagrams

the expected statistical error on m_W, which constitutes the main contribution to the total error and which can be expressed as:

$$\Delta m_W(stat) = \left|\frac{dm_W}{d\sigma_W}\right| \Delta \sigma_W = \left|\frac{dm_W}{d\sigma_W}\right| \sqrt{\sigma_W} \frac{1}{\sqrt{\mathcal{L}}} \frac{1}{\sqrt{\epsilon_W p_W}} \qquad (2)$$

where $\mathcal{L}$ is the luminosity and ϵ_W, p_W are the signal efficiency and purity obtained after the selection. The only dependence on the center of mass energy is contained in the term $|dM_W/d\sigma_W|\sqrt{\sigma_W}$ which has a minimum at $\sqrt{s_{opt}} = 2m_W + 0.5$ GeV $\approx$ 161 GeV [5].

The collider strategy is then to increase center of mass collision energy in several steps. With increased energy the W pair production cross section grows but becomes much less sensitive to m_W, making it impossible to extract the mass from a cross section measurement. However at higher energies Ws are always produced on-shell and it is therefore possible to directly reconstruct their masses.

2.2 background processes

Depending on the boson decay modes, W pair production leads to a final state which can be fully hadronic with four or more jets, partially hadronic with two or more jets and one energetic lepton, or fully leptonic when both Ws decay into one lepton and one neutrino. There are, however, other diagrams which can contribute to the same final states but don't have resonant W bosons. Such diagrams don't carry any information on Ws and are therefore called background diagrams. They can be easily divided into two categories depending on the number of particles in the final state: the so called two fermion background and the four fermion background.

Two fermion processes are basically QED and QCD diagrams which can constitute background for all WW channels. In particular QCD diagrams with two quarks in the final state (with or without initial state radiation) have a cross section between one and two orders of magnitude greater than that of the signal and, in case of gluon emissions in the final state, they can mimic a multi-jet final state very well and are therefore difficult to suppress.
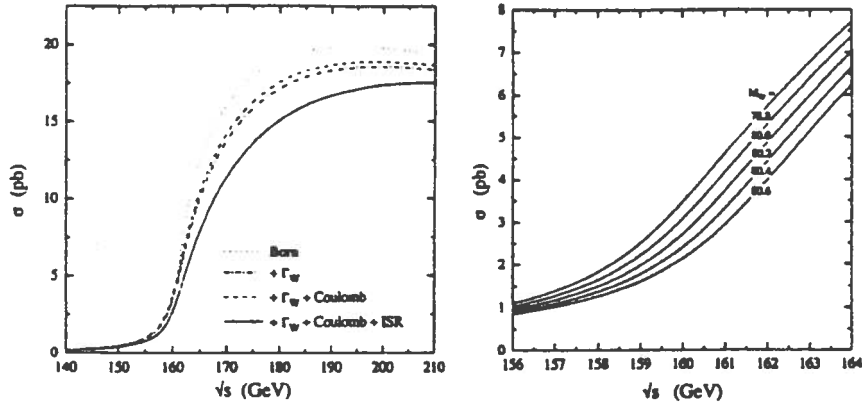
Figure 2: (left) $\sigma^{CC03}(ee \to WW)$ with and without finite width, Coulomb and ISR effects. (right) Complete cross section at threshold with different m_W values.

Four fermion final states include many electroweak diagrams involving either zero, one or two vector bosons. Major contributions to a final state which is similar (or identical) to one coming from CC03 diagrams are given by singly resonant (ee→Weν and ee→Zee) and doubly resonant (ee→ZZ) diagrams. Beacuse their contribution is comparable with that of the CC03 diagrams and they present distinctive characteristics, they can easily be suppressed in the analyses.

3   DELPHI Apparatus and Particle Selection.

Detailed descriptions of the DELPHI apparatus and its performance can be found in references [7], [8]. In 1996 the cylindrical three layer vertex detector was extended with additional silicon strips covering part of the endcap region.

The response of the apparatus to various physics processes was modelled using the full simulation program DELSIM [9] which includes the resolution, granularity and efficiencies of the different detectors.

The particle selection consists of charged and neutral particle selection. Charged particles have to fulfill the following criteria:

- polar angle, defined with respect to the beams direction, between $10°$ and $170°$.

- momentum greater than 0.4 GeV/c and track length greater than 15 cm.

- transverse and longitudinal impact parameter with respect to the beams direction less than 4 cm.

- estimated relative error on the momentum less than 1.

For neutral particles the following criteria were applied

- energy of the shower greater than 0.5 GeV.

- relative uncertainty on the shower energy in the hadron calorimeter less than 1.

Electron identification was performed looking for charged tracks with an associated deposit in a forward or central electromagnetic calorimeter demanding an energy-to-momentum ratio consistent with unity. In the polar region in which electron identification can be applied the identification efficiency was estimated from the simulation to be (.77 ± .02), in good agreement with the value obtained using real Bhabha events.

Muon identification was obtained looking for charged tracks with at least one hit in the muon chambers or only an energy deposition in the hadron calorimeter consistent with a minimum ionizing particle. Within the detector acceptance muon identification efficiency was estimated to be (.92 ± .01) in good agreement with what was obtained using real high energetic muons coming from Z decay or soft muons produced in $\gamma\gamma$ interactions.

4 WW Event Selection.

In this section the selection criteria of WW events are described considering each possible final state. The same criteria have been used at both $\sqrt{s}$ =161 GeV and $\sqrt{s}$ =172 GeV making simple tuning on cuts to account for the energy difference. The selection efficiencies given in the next sections are defined with respect to the doubly W resonant processes defined in figure 1.

4.1 Fully Hadronic Final State.

The Standard Model branching ratio WW→ $q\bar{q}q\bar{q}$ is approximately .46. To select muti-jet topologies the particles are clusterized using the LUCLUS algorithm [10] with d_{join}=6.5 GeV and at least four jets in the event are required. To remove part of the QCD background coming from the radiative return to the Z peak, the effective center of mass energy of the e^+e^- annihilation was calculated using either the energy of a detected isolated photon, if any, or assuming it lost in the beam pipe with momentum extracted from the missing energy in the event. The effective center of mass energy was required to be larger than 115 GeV.

The remaining background contamination corresponds basically to QCD non radiative processes with strong gluon emission in the final state which leads to a multi-jet topology. To partially remove this contribution, all events were then forced into four jets and a constrained fit imposing four-momentum conservation to the event was performed: the final cut at $\sqrt{s}$=161 GeV was then made on the D variable defined as:

$$D = \frac{E_{min}}{E_{max}} \frac{\theta_{min}}{(E_{max} - E_{min})} \tag{3}$$

where E_{min}, E_{max} are the energies of the jets with least and greatest energy and θ_{min} is the smallest interjet angle. The D variable discriminates well between signal and remaining background because WW events consist of two di-jet systems nearly back to back rather balanced in energy, while in $q\bar{q}gg$ events the quark jets

tend to have higher energy and the gluon jets follow the quark directions. The D variable was required to be greater than .013 GeV^{-1}.

At $\sqrt{s}$=172 GeV the cut on D was replaced by a cut on the simpler variable $E_{min}\theta_{min}$, with same notation as before, requiring it to be greater than 680 GeV.

4.2 Mixed Final State.

The decay branching ratio of a W pair in a $q\bar{q}l\nu_l$ system is .44. The selection of $q\bar{q}e\nu_e$ and $q\bar{q}\mu\nu_\mu$ events is easier than that of the fully hadronic channel because of the isolated and energetic lepton present in the final state. More complicated is the identification of $q\bar{q}\tau\nu_\tau$ topologies due to the decay of the τ.

The event was required to have hadronic activity by asking for at least 6 charged tracks in the event and a missing momentum of at least 10 GeV/c caused by the neutrino. The direction of the missing momentum was required to be at least 20° away from the beam pipe direction to remove radiative QCD background. An electron or a muon with an energy greater than 20 GeV and with an isolation angle, defined with respect to the closest charged track with energy above 1 GeV, of at least 10° was then looked for in the event. Also leptons with energy between 10 and 20 GeV but isolation angle of at least 30° were taken into account in order to select some events with a τ decaying leptonically. When no candidate lepton was found, then possible $q\bar{q}\tau\nu_\tau$ topologies with the τ decaying into hadrons were looked for by demanding three jets, one being a low charged ($1\leq N_{ch} \leq 3$) and total ($N_{tot} < 5$) multiplicity jet with small aperture, assessed asking the fraction of the jet energy in a cone of 5° around the jet axis to be above .7.

If one candidate lepton satisfying the described criteria was found, then the remaining part of the event was forced into two jets using the LUCLUS clusterization algorithm.

Four fermion neutral current backgrounds ($q\bar{q}ll$) were then reduced by rejecting events with two detected isolated leptons of the same flavour but with opposite charge. To improve the selection resolution the angle between the candidate lepton (or jet) and the missing momentum was required to be greater than 60° in the muon case or greater than 90° otherwise. To further reduce the $q\bar{q}g$ background in hadronic WW$\rightarrow q\bar{q}\tau\nu_\tau$ events, other loose cuts were applied on the hadronic invariant mass and the effective center of mass energy of the event.

4.3 Fully Leptonic Final State.

The decay branching ratio of a W pair in a $l_1\nu_{l_1}l_2\nu_{l_2}$ system is .10. Events with both Ws decaying leptonically are characterized by two energetic, acoplanar and acollinear leptons with opposite charge and by large missing energy and momentum. The main backgrounds for this channel are QED processes and two photon interactions.

The selection starts with the requirement of low number of tracks in the event ($2\leq N_{ch}^{event} \leq 6$) organized in two jets using LUCLUS with $d_{join} = 5.0$ GeV. In the analysis corresponding to $\sqrt{s}$=161 GeV the momentum of the leading jet was required to lie in the window 20-60 GeV/c and the momentum of the other jet in a
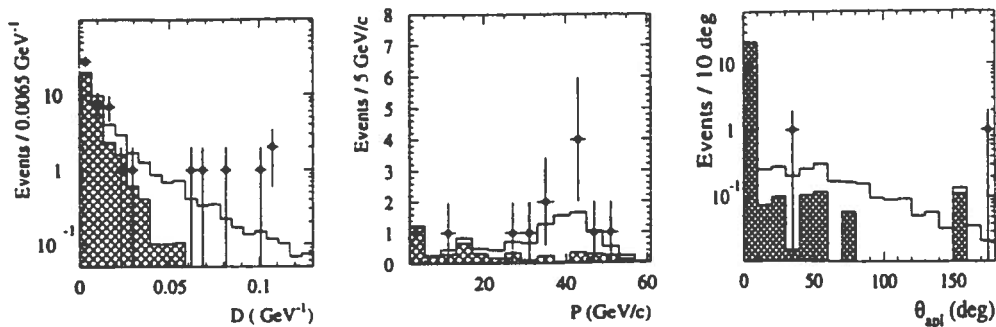
Figure 3: D variable (left, hadronic channel), lepton momentum (center, mixed channel) and aplanarity (right, leptonic channel) distributions. The dots represent the data while the histograms are the MC expectations and are normalized to the number of expected events. The shaded part of the histogram is the contribution of all background. The distributions refer to all the cuts of the analysis being applied except the one on the variable shown.

lower range: 12-50 GeV/c. These intervals were properly rescaled for 172 GeV center of mass energy.

QED radiative background and part of the $\gamma\gamma$ background were rejected by asking the polar angle of the missing momentum to be at least 20°. Two cuts on acollinearity ($\theta_{acol} > 10°$) and acoplanarity ($\theta_{acopl} > 10°$) of the two jets remove most of the Bhabha scattering background and remaining $\gamma\gamma$ interactions.

4.4 Performances.

The selection efficiencies of the criteria described and the background contaminations were obtained using different Montecarlo samples of WW events and background events generated with the PYTHIA generator [10] with the fragmentation tuned to the DELPHI data collected at LEP1. Using different signal samples the selection efficiency was found to be independent of the precise value of m_W in the range from 80.1 to 80.6 GeV/c^2. A crosscheck of the expected number of events was also done using samples generated with EXCALIBUR [11] and were found to be consistent. A detailed summary of the analysis performance and parameters is presented in table 1. Figure 3 shows the distributions of some of the variables described in each channel, comparing the expected signal and background contribution with the data collected.

5 Cross Section Determination.

The W production cross section is a simple function of the number of observed events N_{ev} and the luminosity $\mathcal{L}$:

$$\sigma_W = \frac{N_{ev} - \sigma_{bck}\mathcal{L}}{\epsilon_W \mathcal{L}} \tag{4}$$

where σ_{bck} is the residual background cross section and ϵ_W the efficiency on the signal. The partial cross sections are determined using a maximum likelihood with

	$q\bar{q}q\bar{q}$	$q\bar{q}l\nu_l$	$l\nu_l l\nu_l$	$\sqrt{s}$
$\epsilon(\%)$	61.3 ± 2.0	60.9 ± 3.0	47.7 ± 3.0	
σ_{bck}(pb)	$.61 \pm .07$	$.19 \pm .02$	$.06 \pm .04$	
$\mathcal{L}$(pb^{-1})	9.93	9.69	9.93	161 GeV
$Events$	15	12	2	
σ_W(pb)	$1.56^{+.67}_{-.55} \pm .13$	$1.77^{+.67}_{-.55} \pm .10$	$.31^{+.39}_{-.24} \pm .09$	
$\epsilon(\%)$	75.5 ± 0.7	57.0 ± 1.0	47.6 ± 1.4	
σ_{bck}(pb)	$1.58 \pm .07$	$.19 \pm .04$	$.06 \pm .05$	
$\mathcal{L}$(pb^{-1})	9.98	9.98	9.98	172 GeV
$Events$	55	34	3	(prel.)
σ_W(pb)	$5.21^{+1.03}_{-.95}$	$5.64^{+1.09}_{-.97}$	$.52^{+.45}_{-.30}$	

Table 1: Summary of efficiencies, background cross sections, luminosities collected, number of events observed and extracted cross sections at the two different center of mass energies divided per channel. The errors at $\sqrt{s}$=161 GeV already include systematic effects.

a poissonian probability where the number of expected events is parametrized by σ_W according to the previous relation. To extract the total cross section the same method is used and the Standard Model branching ratios are assumed.

Table 1 shows the extracted cross sections per channel. Combining the numbers as described, the following values are obtained for the W pair production cross sections:

$$\sigma(ee \rightarrow WW, \sqrt{s} = 161 \text{ GeV}) = 3.67^{+.97}_{-.85} \ (stat) \pm .19 \ (syst) \text{ pb}$$
$$\sigma(ee \rightarrow WW, \sqrt{s} = 172 \text{ GeV}, \ prel.) = 11.38^{+1.54}_{-1.43} \ (stat) \pm .32 \ (syst) \text{ pb}$$

where the systematic errors take into account uncertainties coming from selection efficiencies, background cross sections, luminosity, hadronization modelling and lepton misidentification. Figure 4 shows the two values compared with the Standard Model expectations.

6 m_W Determination.

6.1 m_W at Threshold.

The value of m_W at threshold is determined from the measured value of the CC03 cross section. The interference terms between the CC03 processes and other electroweak diagrams which give identical final states can be seen as a correction factor, which is used to get the CC03 cross section from the data. The correction factors were determined for each decay mode using the four fermion generator EXCALIBUR interfaced to DELSIM and are presented in table 2.

The mean LEP center of mass energy at DELPHI was determined to be 161.31 GeV with an error of 50 MeV [12]. Figure 5 shows the dependence of σ_W^{CC03} from
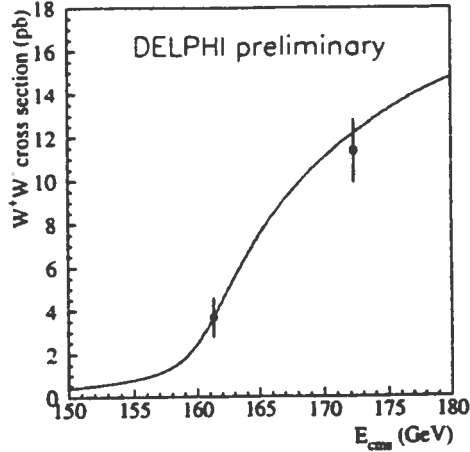
Figure 4: DELPHI measurements of WW production cross sections at the center of mass energies of 161.3 and 172.3 GeV compared with Standard Model prediction using $m_W = 80.36 \text{ GeV}/c^2$.

WW final state	CC03 corr.
$q\bar{q}q\bar{q}$	0.996
$q\bar{q}e\nu_e$	1.087
$q\bar{q}\mu(\tau)\nu_{\mu(\tau)}$	1.006
$l\nu_l l\nu_l$	1.045

Table 2: CC03 correction factors. The relative uncertaintes on the different factors was estimated to be about 1.5 %.

m_W with $\sqrt{s}$ fixed to the measured value. The curve is obtained using the program GENTLE [13] (version 2.0) and allows a determination of the W boson mass from the cross section, leading to the value:

$$m_W = 80.40 \pm 0.44 \, (stat) \pm 0.09 \, (syst) \pm 0.03 (LEP) \text{ GeV}/c^2 \quad (5)$$

where the systematic error includes the theoretical uncertainties on the CC03 cross section and the last error corresponds to the LEP center of mass energy error.

6.2 m_W at $\sqrt{s}$=172 GeV.

With increased energy, the two Ws in the event are always on shell and it is therefore possible to fully reconstruct the resonances from their decay products. This procedure cannot be applied to the fully leptonic channel because of the two missing neutrinos.

In order to improve the energy resolution in the event, made worse by undetected particles, detector imperfections and topology of the event itself, a constrained kinematic fit using the fourmomenta of the jets and the lepton was performed. The fit was done imposing energy and momentum conservation and equality of the masses of the two Ws. In the mixed hadronic channel the momentum of the neutrino was
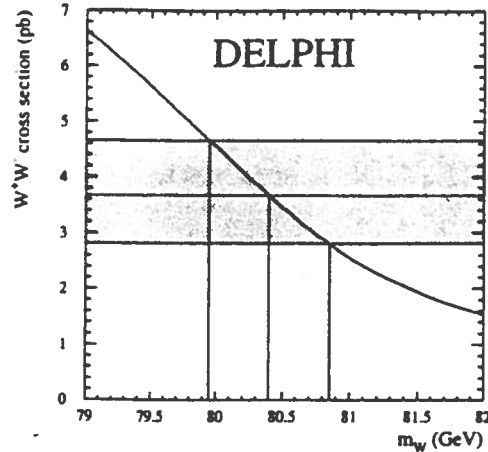
Figure 5: CC03 cross section at $\sqrt{s}$=161.31 GeV versus m_W and the DELPHI result, where the shaded band corresponds to one standard deviation variation of the measurement.

assumed equal to the missing momentum.

In figure 6 the reconstructed fully hadronic and mixed hadronic W mass spectra are shown. Moreover, a second approach was used in the hadronic channel: after a simple rescaling of the energies of the di-jet systems, the mass was calculated using simply the directions of the jets, less sensitive to detector resolution effects.

The extraction of the mass from the spectra was done with an unbinned maximum likelihood fit to the distributions, using as probability density function a Breit-Wigner convoluted with a resolution gaussian to describe the signal and a constant term to describe the background. In the hadronic channel the ideogram technique was also used [14] in order to take correctly into account all three pairings that are possible in a four jets system to build two invariant masses.

The results were corrected for biases and linearity effects studied on Montecarlo samples. The results obtained in the hadronic channel were then combined, taking into account the correlations between the two methods. They were then combined with the result in the mixed hadronic channel. The preliminary DELPHI result on m_W measured with direct reconstruction is:

$$m_W = 79.95 \pm 0.38 \ (exp) \pm 0.05 \ (fsi) \pm 0.03(LEP) \ \text{GeV}/c^2 \qquad (6)$$

where the first error includes the statistical error and the systematics coming from background modelling, linearity and jet/lepton energy uncertainties. The second error concerns the unknown effect of final state interaction, such as color reconnection between quarks [5] and Bose Einstein correlation between identical particles coming from the decay of different Ws [15], [5]. The last error comes from the LEP beam energy uncertainty.
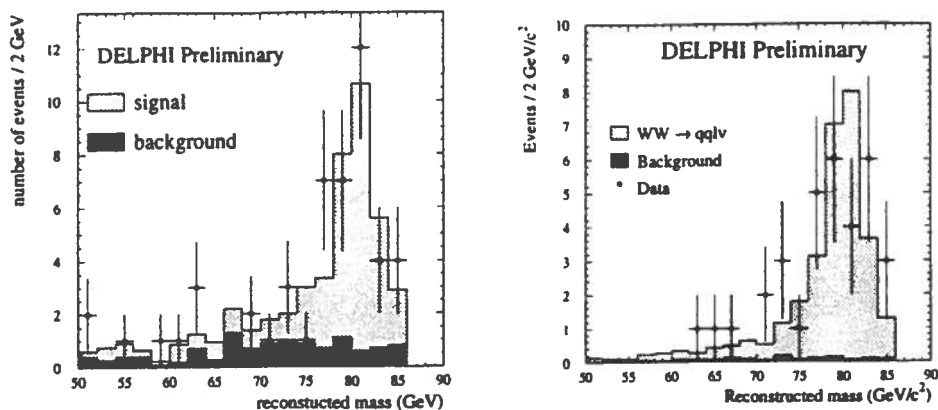
Figure 6: Hadronic and semileptonic mass spectra at $\sqrt{s}$ =172 GeV.

6.3   Combination of Results.

Combining the results obtained at threshold energy and at a center of mass energy of 172 GeV gives the preliminary DELPHI result for the W boson mass:

$$m_W = 80.14 \pm 0.29 \ (exp) \pm 0.03 \ (fsi) \pm 0.03(LEP) \ \text{GeV}/c^2 \qquad (7)$$

where the conventions are the same as above.

7   Summary and Outlook.

During 1996, DELPHI detector collected a total luminosity of approximately 20 pb^{-1}. For the first time at e^+e^- accelerators, W boson production was observed and studied.

The W$^-$W$^+$ production cross section and the W mass were determined at both center of mass energies of 161 GeV and 172 GeV. All numbers obtained were found to be consistent with the Standard Model predictions.

Combining the mass measurements, DELPHI obtained a preliminary value for m_W of 80.14 GeV/c^2 with an experimental error of 0.29 GeV/c^2. The combination of all LEP2 collaborations results yields the preliminary value, shown in figure 7 together with the Tevatron result, of:

$$m_W(LEP, prel.) = 80.38 \pm 0.14(exp) \ \text{GeV}/c^2 \qquad (8)$$

With only a small fraction of the total luminosity foreseen for LEP2, the result is already competitive with the one coming from $p\bar{p}$ accelerators. The present world average value becomes:

$$m_W(WORLD, prel.) = 80.37 \pm 0.08(exp) \ \text{GeV}/c^2 \qquad (9)$$

The future high-luminosity LEP runs before the year 2000 at $\sqrt{s}$ = 184 GeV and $\sqrt{s}$ = 192 GeV will allow a much more precise determination of the W boson mass: the aim is to reach, or even exceed, the accuracy of 40 MeV/c^2 with which m_W is
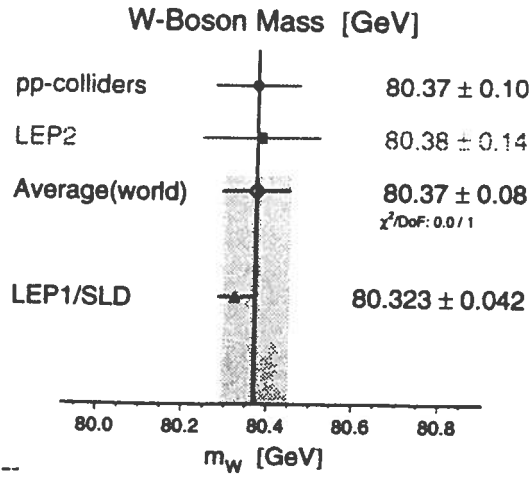
Figure 7: Status of m_W measurement. The present world average is reported, together with the number obtained by the electroweak fit using both LEP1 and SLD data.

predicted by the present fit to all electroweak parameters coming from LEP1 and SLD data and therefore to be able to make a new, stringent test of the validity of the Standard Model.

References

[1] UA2 Collaboration, Phys. Lett. **B276** (1992) 354.

[2] CDF Collaboration, Phys. Rev. Lett. **75** (1995) 11.

[3] D0 Collaboration, Phys. Rev. Lett. **77** (1996) 3309.

[4] M. Rijssenbeek, *W mass from the Tevatron*, FERMILAB CONF-96/365-E, to appear in the proceedings of the 28th International Conference on High Energy Physics, Warsaw, 25-31 July 1996.

[5] Z. Kunst, W. J. Stirling *et al*, *Determination of the Mass of the W Boson*, eds. G. Altarelli, T. Sjöstrand and F. Zwirner, CERN 96-01 (1996) Vol.1, 141-205.

[6] W. Beenakker, F. A. Berends *et al*, *WW Cross Sections and Distributions*, eds. G. Altarelli, T. Sjostrand and F. Zwirner, CERN 96-01 (1996) Vol.1, 79-134.

[7] DELPHI Collaboration, Nucl. Instr. & Meth. **A303** (1991), 233.

[8] DELPHI Collaboration, Nucl. Instr. & Meth. **A378** (1996), 57.

[9] DELPHI Collaboration, *DELPHI Event Generation and Detector Simulation - User Guide*, DELPHI Note 89-67 (1989), unpublished.

[10] T.Sjöstrand, *PYTHIA 5.7 / JETSET 7.4*, CERN-TH 7112/93 (1993)

[11] F. A. Berends, R. Kleiss, R. Pittau, *EXCALIBUR*, eds. G. Altarelli, T. Sjostrand and F. Zwirner, CERN 96-01 (1996) Vol.2, 23-26.

[12] LEP Energy Working Group, *LEP Energy Calibration in 1996*, LEP Enrgy Group 97-01 (1997).

[13] D. Bardin *et al*, *GENTLE*, eds. G. Altarelli, T. Sjostrand and F. Zwirner, CERN 96-01 (1996) Vol.2, 26-30.

[14] M. Bigi *et al*, *Measurement of the Mass of the W Boson Using Direct Reconstruction*, DELPHI Note 97-20 (1997), unpublished.

[15] DELPHI Collaboration, *Measurement of Correlations between Pions from Different Ws in $e^+e^- \rightarrow W^+W^-$ Events* PPE 97–30 (1997). Submitted to Phys. Lett. B